Published in final edited form as:
Mol Cancer Ther. 2008 September ; 7(9): 2662–2671. doi:10.1158/1535-7163.MCT-08-0136.

Pomegranate extract inhibits androgen-independent prostate cancer growth through a nuclear factor-κB-dependent mechanism

Matthew B. Rettig[1,2,5], **David Heber**[4], **Jiabin An**[5], **Navindra P. Seeram**[4], **Jian Y. Rao**[3], **Huiren Liu**[1], **Tobias Klatte**[2], **Arie Belldegrun**[2], **Aune Moro**[4], **Susanne M. Henning**[4], **Deqiong Mo**[5], **William J. Aronson**[2,6], and **Allan Pantuck**[2]

[1] Department of Medicine, Division of Hematology-Oncology, David Geffen School of Medicine at University of California-Los Angeles

[2] Department of Urology, David Geffen School of Medicine at University of California-Los Angeles

[3] Department of Pathology, David Geffen School of Medicine at University of California-Los Angeles

[4] Center for Human Nutrition, David Geffen School of Medicine at University of California-Los Angeles

[5] Department of Medicine, VA Greater Los Angeles Healthcare System-West Los Angeles, Los Angeles, California

[6] Department of Urology, VA Greater Los Angeles Healthcare System-West Los Angeles, Los Angeles, California

Abstract

Constitutive nuclear factor-κB (NF-κB) activation is observed in androgen-independent prostate cancer and represents a predictor for biochemical recurrence after radical prostatectomy. Dietary agents such as pomegranate extract (PE) have received increasing attention as potential agents to prevent the onset or progression of many malignancies, including prostate cancer. Here, we show that PE inhibited NF-κB and cell viability of prostate cancer cell lines in a dose-dependent fashion *in vitro*. Importantly, maximal PE-induced apoptosis was dependent on PE-mediated NF-κB blockade. In the LAPC4 xenograft model, PE delayed the emergence of LAPC4 androgen-independent xenografts in castrated mice through an inhibition of proliferation and induction of apoptosis. Moreover, the observed increase in NF-κB activity during the transition from androgen dependence to androgen independence in the LAPC4 xenograft model was abrogated by PE. Our study represents the first description of PE as a promising dietary agent for the prevention of the emergence of androgen independence that is driven in part by heightened NF-κB activity.

Introduction

A large body of literature has linked inflammation to prostate carcinogenesis. Areas of chronic inflammation are almost universally present in pathologic specimens of the prostate,

Requests for reprints: Matthew B. Rettig, Department of Medicine, VA Greater Los Angeles Healthcare System-West Los Angeles, Building 304, Room E1-113, 11301 Wilshire Boulevard, Los Angeles, CA 90073. Phone: 310-268-3622; Fax: 310-268-4508. mrettig@mednet.ucla.edu.

Disclosure of Potential Conflicts of Interest

A. Pantuck, grant support from POM Wonderful and Sence Foundation. No other potential conflicts of interest were disclosed.

including biopsy cores, transurethral resection chips, and total prostatectomy specimens. In one series, a 98% incidence of inflammatory lesions was observed in 162 surgically resected hyperplastic prostates (1). The prostatic lesion known as proliferative inflammatory atrophy occurs at sites of chronic inflammation and is frequently found in association with and adjacent to prostate intraepithelial neoplasia and prostate cancer in patient specimens (2). Based on spatial association and on genetic and protein expression analyses, proliferative inflammatory atrophy has been proposed as a precursor to prostatic intraepithelial neoplasia and prostate cancer.

One of the most well-established signaling pathways mediating inflammatory responses relevant to cancer is the nuclear factor-κB (NF-κB) pathway. NF-κB represents a family of transcription factors that modulate expression of genes with diverse functions. The activity of NF-κB is regulated by the inhibitor of κB (IκB), the NF-κB-inhibitory protein that binds to and sequesters NF-κB family members in the cytoplasm. When the NF-κB pathway is activated, IκB is phosphorylated by IκB kinase, which phosphorylates IκB at serine residues 32 and 36 (3). Phosphorylated IκB is subjected to ubiquitination and proteasome-mediated degradation, which results in the translocation of NF-κB to the nucleus, where it functions as a transcription factor.

Constitutive NF-κB activation has been observed in breast cancer, liver cancer, melanoma, Hodgkin's disease, and cervical cancer (3–6). Direct genetic evidence in murine models of colon and liver cancer have established that NF-κB activation within tumor cells or infiltrating inflammatory cells is required for tumor initiation or promotion (7,8). Importantly, constitutive activation of NF-κB in primary prostate cancer specimens is observed and represents an independent risk factor for recurrence after radical prostatectomy (9,10).

Pomegranate ellagitannins, a group of bioactive constituents of pomegranate juice (PJ) derived from the *Punica granatum* fruit, have received increasing attention for their potential as nontoxic chemopreventive dietary agents. Our group recently showed that consumption of PJ produced from pressed whole pomegranate fruit prolonged the doubling time of the serum prostate-specific antigen (PSA) tumor marker in patients who had experienced a PSA recurrence after prostatectomy (11). Interestingly, pomegranate extract (PE) has been shown to inhibit NF-κB in normal human cells, including chondrocytes, epidermal keratinocytes, and vascular endothelial cells (12–14). To our knowledge, the ability of PE to inhibit NF-κB in prostate cancer models has not been reported. Similarly, the role of the NF-κB-inhibitory effects of PE on prostate cancer growth has not been investigated. Here, we show that PE inhibits NF-κB both *in vitro* and *in vivo* in prostate cancer models and that this NF-κB inhibitory is required for the maximal proapoptotic effect of PE. Moreover, PE delays the emergence of androgen independence in the LAPC4 prostate cancer murine xenograft model.

Materials and Methods

Cell Culture and Prostate Cancer Cell Lines

LNCaP-AR and LAPC4 cells (a gift from Dr. Charles Sawyers, University of California-Los Angeles) were maintained in RPMI 1640 supplemented with 10% fetal bovine serum and penicillin (100 μg/mL) and streptomycin (100 μg/mL). LNCaP-AR is a version of the parental LNCaP cells that not only expresses its own endogenous version of the androgen receptor (AR) but also is stably transfected with wild-type AR, so that the net effect is overexpression of the AR that is sufficient to recapitulate the androgen-independent state (15). CL1 cells represent an androgen-independent subclone of LNCaP that was generated by culturing LNCaP in charcoal-stripped, androgen-depleted serum, as described (16). CL1

cells were maintained as for LNCaP cells but continuously in charcoal-stripped serum. DU145 cells (American Type Culture Collection) were maintained in DMEM containing 10% fetal bovine serum and antibiotics.

Reagents

Recombinant human tumor necrosis factor-α (TNF-α; R&D Systems) was dissolved in PBS. A κB-responsive plasmid (p4x-κB-luc) in which four copies of the κB-response element drives expression of firefly luciferase was purchased from Invitrogen. The pRL-SV40 plasmid, in which *Renilla* luciferase is constitutively expressed under the regulation of the SV40 promoter/enhancer, was purchased from Promega and was used for normalization of firefly luciferase activity. A firefly reporter construct driven by the *PSA* promoter/enhancer (*PSA*-P/E-luc) was a kind gift of Dr. Michael Carey (University of California-Los Angeles School of Medicine). The pEGFP-p65 [enhanced green fluorescent protein (EGFP) fused in-frame to the NH_2 terminus of p65] and pCMV-p50 expression plasmids were described previously (17).

Pomegranate Formulations

For our studies, we employed two pomegranate formulations: PJ and PE. PE is a standardized extract (POMX; POM Wonderful) of pomegranate fruit grown in California (*P. granatum* L., Wonderful variety; Paramount Farms). PE is made from fruit skins standardized to ellagitannins, as punicalagins (37–40%), and free ellagic acid (3.4%) as determined by high-performance liquid chromatography using previously described methods (18). PE was administered to animals in doses based on the amount of ellagitannins in a single serving of PJ (240 mL single-strength juice, 80 mg of ellagitannins, as punicalagins; ref. 18). The equivalent dose that would be administered to a 70 kg human was calculated for a mouse of 25 g body weight to be 0.03 mg ellagitannins. Ten times this dose was used in the animal studies (0.8 mg PE/dose/animal). PE was suspended in 10% aqueous glucose solution for oral administration.

PJ (POM Wonderful) was used as a concentrate that contains the following polyphenols: 1,561 mg/L punicalagins, 121 mg/L ellagic acids, 387 mL/L anthocyanins, and 417 mg/L other hydrolysable tannins, as described (18).

Transient Transfections and Reporter Gene Assays

Cells were plated at 10^5 per well in 24-well plates the day before transfection. The plasmids were transfected with LipofectAMINE Plus (Life Technologies) according to the manufacturer's instructions. Protein was extracted 48 h after transfection, and firefly and *Renilla* luciferase were measured on a TD20/20 tube luminometer (Turner Designs) using a Dual Luciferase Assay kit (Promega) according to the manufacturer's instructions. Firefly luciferase activity was normalized to *Renilla* luciferase expression.

Cell Viability, Apoptosis, and Cell Cycle Analyses

LNCaP, LAPC4, CL1, and DU145 cells were seeded in 96-well plates the day before chemical treatment at concentrations of 4×10^4, 4×10^4, 1×10^4, and 2×10^4 per well, respectively. Cell viability was measured by the methylene blue assay (19). All experiments were done in quadruplicate. Relative cell viability was calculated by normalizing methylene data to that of the respective untreated samples.

Apoptosis was measured with an Annexin V-FITC staining kit (BD Biosciences) according to the manufacturer's instructions; cells were analyzed on a Becton Dickinson FACSCalibur flow cytometer with CellQuest software (BD Biosciences). Cell cycle analysis was done by hypotonic propidium iodide staining, as described (17).

For experiments to determine the effects of ectopic expression of p65/p50 on PE-induced apoptosis, cells were transiently transfected with pEGFP-p65 and pCMV4-p50 or the parental control vectors. Twenty-four hours after transfection, PE was added for an additional 24 h. Apoptosis was measured on EGFP-positive cells using a terminal deoxynucleotidyl transferase-mediated dUTP nick end labeling (TUNEL) assay kit (*In situ* Cell Death Detection kit, TMR Red; Roche Molecular Biomedicals) by flow cytometry.

Xenograft Model

All mice received a standard research diet (AIN 93G; Dyets) *ad libitum* throughout the experiment. Androgen-dependent LAPC4 prostate cancer cells (2×10^6; C. Sawyers, Department of Medicine, University of California at Los Angeles) were implanted s.c. into the shoulders of 5-week-old severe combined immunodeficient mice (Taconic Farms). When tumors became palpable 2 weeks after tumor cell injection, mice were administered either PE ($n = 9$ mice) or vehicle control ($n = 18$ mice) orally5 days/wk (Monday–riday). Oral dosing was accomplished by gently securing the mouse with one hand and delivering the PE or vehicle control via an animal feeding needle (Biomedical Needles, Popper and Sons) attached to a 1 mL tuberculin syringe. Tumors were measured twice weekly and mice were weighed weekly. One week after initiation of oral dosing, nine mice each from the PE and vehicle control groups were castrated. All mice were maintained on their assigned treatment group for an additional 2 weeks after the castration date. Tumor volumes were calculated using the formula: length × width × height × 0.5236 (18), and mice in both groups were sacrificed when tumors in either group reached 1 cm in maximum dimension. At sacrifice, primary tumors were excised and weighed, blood was collected by cardiac puncture, and serum was obtained by centrifugation at 3,000 × *g* for 10 min at 4°C. All animal protocols were approved by University of California-Los Angeles Chancellor's Animal Care and Use Committee.

Measurement of Serum PSA

Serum PSA at the time of sacrifice was measured with a PSA ELISA kit (Diagnostic Systems Laboratories) according to the manufacturer's instructions.

Immunohistochemistry

Detection of Apoptosis—Formalin-fixed, paraffin-embedded tissue sections were dewaxed with xylene and ethanol according to standard procedures. The apoptotic cell death was detected in the cell preparations by the TUNEL method using the *In Situ* Cell Death Detection Kit, AP (Boehringer Mannheim). The slides were put in a glass jar containing 500 mL of 0.01 mol/L (pH 6.0) citrate buffer at 95°C for antigen retrieval for 5 min and then transferred to 0.3% H_2O_2 in methanol for 5 min. Then, the slides were incubated with freshly prepared 3% bovine serum albumin blocking solution for 30 min at room temperature. After three rinses with PBS, the slide was incubated with 50 μL TUNEL reaction mixture for 60 min at 37°C. Subsequently, the slides were further incubated with 50 μL Converter-AP on section for 30 min at 37°C and with 50 μL substrate solution for 10 min at room temperature. The slides were then counterstained with hematoxylin and mounted with glass coverslips for light microscopic examination.

Ki-67 Staining for Proliferation—Formalin-fixed, paraffin-embedded tissue sections were dewaxed with xylene and ethanol according to standard procedures. Antigen retrieval was done in a 0.01 mol/L sodium citrate buffer (pH 6.0) in a heater at 100°C for 10 min. Slides were then washed with 1× PBS and treated with 3% H_2O_2 for 10 min and washed again with 1× PBS. Slides were blocked with avidin and biotin in 5% serum at room temperature for 30 min and then incubated with a Ki-67 primary antibody

(DakoCytomation) at room temperature for 1 h. Slides were washed with 1× PBS and incubated with biotinylated anti-mouse secondary antibody (DakoCytomation) for 30 min at room temperature. Slides were then washed and incubated with Strept ABComplex kit (DakoCytomation) for 15 min. Slides were washed and incubated with the DAB Substrate-Chromogen Systemstain (DakoCytomation) for 1 to 5 min. Slides were then counterstained with hematoxylin and mounted with glass coverslips for light microscopic examination.

Electrophoretic Mobility Shift Assays

Wild-type and mutant κB oligonucleotide probes were purchased from Santa Cruz Biotechnology. Nuclear protein (15 μg) was combined with end-labeled, double-stranded κB oligonucleotide probe, 1 μg poly-dIdC (Amersham Pharmacia Biotech), 1 μg bovine serum albumin, and 5 mmol/L spermidine in a final reaction volume of 20 μL for 20 min at room temperature. The DNA protein complex was run on a 4% nondenaturing polyacrylamide gel with 0.4× TBE running buffer before subsequent autoradiography. Cold competition experiments were done with a 100-fold molar excess of cold wild-type or cold mutant κB oligonucleotides. For supershift assays, nuclear protein was preincubated with specific or control antibodies (6 μg; purchased from Santa Cruz Biotechnology) for 20 min at room temperature. An identical strategy was employed for electrophoretic mobility shift assays (EMSA) with Oct-1 probes as a specificity control for the effects of PE.

Results

Inhibition of NF-κB by PE *In vitro*

Our first goal was to test the ability of PE to inhibit constitutive and TNF-α-induced NF-κB activity. As shown in Fig. 1A, PE inhibited constitutive NF-κB activity in androgen-independent DU145 cells in a dose-dependent fashion. Because DU145 cells exhibit high constitutive NF-κB activity, we were also able to document the NF-κB-inhibitory effect of PE by EMSA (Fig. 1B, *top*, *lanes 1–5*). Cold competition experiments with excess cold wild-type and cold mutant κB probes showed the specificity of the shifted bands (Fig. 1B, *top*, *lanes 11* and *12*). PE did not affect the electrophoretic mobility of the Oct-1 transcription factor (Fig. 1B, *bottom*), a finding that establishes that PE does not exhibit generalized inhibition of transcription factor-DNA interactions.

Next, we assessed the ability of PE to block NF-κB activity induced by the inflammatory cytokine, TNF-α. PE inhibited TNF-α-induced NF-κB activation as determined by EMSA in the androgen-independent DU145 and CL1 cell lines (Fig. 1B, *lanes 6–10*, and C, respectively). As a complementary assessment of the effects of PE on TNF-α-induced NF-κB activation, we assessed the levels of IκBα, the NF-κB-inhibitory protein that is degraded on activation of the NF-κB pathway. Whereas TNF-α resulted in an expected decrease in IκBα protein expression, exposure of DU145 and LAPC4 cells to PE led to a time-dependent increase in IκBα levels (Fig. 1D). Thus, our initial studies established that PE can effectively block both constitutive and TNF-α-induced NF-κB activity.

Prostate Cancer Growth Inhibition *In vitro* by PE Is Dependent on Inhibition of NF-κB

We evaluated the PE-mediated growth-suppressive effects on prostate cancer cells *in vitro*. We initially focused on the DU145 cell line because it manifests constitutive NF-κB activation. We compared the efficacy of PJ versus PE at various dilutions (see Materials and Methods for preparation juice versus extract). Across all dilutions, PE more effectively inhibited overall growth of DU145 cells than did the PJ (Fig. 2A and B). Consequently, for subsequent cell viability studies, PE was used.

We next examined whether cell growth inhibition was attributable to inhibition of apoptosis. Indeed, PE exposure resulted in a dose-dependent induction of apoptosis in DU145 cells as measured by flow cytometric analysis of Annexin V-stained cells (Fig. 3A). Moreover, PE treatment led to a reduction in S-phase fraction and an accumulation of cells in the G_1 phase (Fig. 3B) in the DU145 model, a finding that indicates that PE may suppress growth not only by induction of apoptosis but also by inhibition of proliferation.

To determine whether the NF-κB-inhibitory effect of PE was involved in the proapoptotic effects of PE, we employed a strategy to maintain NF-κB activation in the presence of PE. Thus, if NF-κB inhibition is required for PE-induced apoptosis, then maintaining NF-κB activation in the presence PE ought to abrogate the proapoptotic effects of PE. To maintain NF-κB activity during PE exposure, we transiently transfected DU145 cells with NF-κB family member expression vectors, p65 and p50 (pEGFP-p65 and pCMV-p50, respectively), and measured NF-κB activity by cotransfecting a *PSA* promoter/enhancer-luciferase reporter (*PSA*-P/E-luc). In addition to androgen response elements, the *PSA* promoter contains four NF-κB *cis*-acting elements (so-called κB sites). Because DU145 cells lack AR expression (20), *PSA* promoter activity in DU145 cells is not principally governed by AR activity but is in large part mediated by NF-κB activity.

We initially identified combinations of quantities of transfected pEGFP-p65 and pCMV-p50 DNA and concentrations of PE that yielded *PSA* promoter/enhancer-driven reporter gene expression that approximated that of control vector-transfected and PBS-treated cells. As shown in Fig. 4A, transfection of 0.5 μg of each of the pEGFP-p65 and pCMV-p50 expression vectors in the presence of PE at 1:1,000 and 1:2,000 dilutions resulted in *PSA* promoter/enhancer-driven reporter gene expression equivalent to that of the DU145 control cells (cells transfected with empty vector controls and PBS). Similar results were obtained when we substituted the *PSA*-P/E-luc vector with a reporter vector that contains three tandem copies of the consensus κB response element (data not shown).

Having identified the transfection conditions to preserve the basal level of NF-κB in the presence of PE, we tested DU145 cells transfected with the pEGFP-p65 and pCMV-p50 or control vectors for PE-induced apoptosis. Twenty-four hours after transfection, cells were exposed to PE or vehicle control for an additional 24 h. Apoptosis of EGFP-positive cells was analyzed by flow cytometry with a TUNEL assay that uses tetramethylrhodamine red (Texas red) as the fluorochrome. Compared with control transfected cells, EGFP-p65/p50-transfected cells showed reduced PE-induced apoptosis. For example, at a PE dilution of 1:1,000, 65.4% of control transfected cells underwent apoptosis compared with 11.5% of EGFP-p65/p50-transfected DU145 cells. Similarly, control transfected cells experienced a greater degree of apoptosis at a PE dilution of 1:1,000. These results indicate that the maximal proapoptotic effect of PE is dependent on the NF-κB-inhibitory effect of PE.

PE has been shown to affect the activity of multiple signaling pathways (21). Indeed, the fact that preservation of NF-κB activity by transfection of p65 and p50 did not completely abrogate PE-induced apoptosis indicates that NF-κB-independent pathways are operative. This notion is supported by (*a*) our finding that PE inhibited the *in vitro* growth of androgen-sensitive (LAPC4) and androgen-independent (CL1 and LNCaP-AR) cell lines that lack basal NF-κB activity in a dose-dependent fashion (Fig. 4C) and (*b*) our recent report that PE can inhibit the growth of androgen-dependent prostate cancer xenografts that do not manifest constitutive NF-κB activity (22).

PE Inhibits Growth of Androgen-Independent LAPC4 Xenografts

To more fully characterize the effects of PE on prostate cancer cells that exhibit endogenous NF-κB activity, we used LAPC4 murine xenografts that develop in a castrate milieu. As

murine xenografts, LAPC4 tumors are androgen dependent, cease growth on castration, and subsequently regrow after a latency of several weeks as androgen-independent tumors (23). In addition and as reported previously (20), LAPC4 cells exhibit constitutive NF-κB activity on emergence of the androgen-independent state. Thus, the LAPC4 xenograft model represents a reasonable recapitulation of the clinical response to androgen deprivation and a suitable system to determine whether PE can inhibit NF-κB *in vivo*.

We established LAPC4 xenografts in the flanks of intact male severe combined immunodeficient mice. When tumors became palpable, mice were fed either PE or vehicle control. One week later, animals were castrated. Importantly, the tumors in the castrate/PE group displayed significantly delayed growth compared with the castrate vehicle control group (Fig. 5A). Specifically, tumors in the control group grew despite castration, whereas PE treatment prevented the regrowth observed after castration. That is, PE inhibited androgen-independent growth. Whereas the mean tumor volume at sacrifice in the control animals was 250 ± 100 mm^3, the mean volume in the PE group was only 88 ± 23 mm^3. Similarly, serum PSA values were lower in the PE group (Fig. 5B). Moreover, animals in the PE group displayed no adverse affects (e.g., weight loss, decreased appetite, or diminished activity) of PE treatment. Mice were weighed weekly, and no differences in weight were observed in the control and PE-treated groups. Thus, PE manifests growth-suppressive effects in this castration model of androgen-independent prostate cancer.

To more fully elucidate the mechanism of growth suppression *in vivo*, we did immunohistochemical studies on formalin-fixed, paraffin-embedded xenografts harvested from the castrate/PBS and castrate/PE groups. We found that the PE diet reduced the staining for Ki-67 (Fig. 5C and D), a proliferation marker. In addition, PE also increased apoptosis as measured by TUNEL staining (Fig. 5C and D). Thus, PE retards the *in vivo* growth of prostate cancer xenografts through a combination of inhibition of proliferation and induction of apoptosis.

Given the established inhibitory effects of PE on NF-κB *in vitro*, we examined whether PE also blocks the NF-κB activation induced during the transition from androgen dependence to androgen independence. Using nuclear protein extracts from LAPC4 xenografts, we showed that NF-κB activity increases in the tumors isolated from castrated/vehicle compared with intact/vehicle mice (Fig. 6A), a finding that has been reported previously (20). More importantly, in the castrated/PE group, the NF-κB activity was markedly reduced compared with the castrated/vehicle group (Fig. 6A). As a complementary assay, we did Western blots for phospho-IκBα. As shown in Fig. 6B, tumors from castrate animals fed PE versus vehicle showed reduced phospho-IκBα levels, which corroborates our EMSA findings and establishes the efficacy of PE to inhibit NF-κB activity *in vivo*.

Discussion

We have shown that PE inhibits constitutive and cytokine-stimulated NF-κB activity in prostate cancer cells *in vitro*. Importantly, the NF-κB-inhibitory effect of PE was necessary for the maximal proapoptotic effect of PE. In addition, we showed that PE not only inhibited the NF-κB activation that occurs in the context of androgen independence of LAPC4 xenografts but also delayed the emergence of androgen independence in the LAPC4 xenograft model. This biological effect is mediated by reduced proliferation and heightened apoptosis. Previous work by our group showed that PE also inhibits angiogenesis in prostate cancer xenografts (24). However, the fact that PE retards the growth of androgen-dependent LAPC4 xenografts (22) as well as *in vitro* growth of prostate cancer cells that lack constitutive NF-κB activation implicates NF-κB-independent effects of PE.

Our results are in line with the accumulation of evidence that points to a pathophysiologic role for NF-κB in prostate cancer progression. Constitutive activation of NF-κB is observed and represents an independent risk factor for recurrence after radical prostatectomy (9,10). Compared with benign prostate tissue, basal NF-κB activation is detected in low- and high-grade prostate cancer clinical specimens and is associated with the expression of NF-κB-regulated gene products including Bcl-2, cyclin D1, matrix metalloproteinase-9, and vascular endothelial growth factor (25). Constitutive NF-κB activation is also observed in human prostate cancer cell lines and xenograft models (26–28). A progressive increase in NF-κB activity occurs during prostate cancer oncogenesis in the transgenic adenocarcinoma of mouse prostate model (29). Pharmacologic or genetic inhibition of NF-κB results in decreased invasion, angiogenesis, clonogenicity, tumorogenicity, and metastasis in multiple preclinical *in vitro* and *in vivo* prostate cancer models (26,30–34). NF-κB blockade also sensitizes to various cytotoxic stimuli, such as TNF-α (31). Moreover, greater constitutive NF-κB activation is consistently observed in androgen-independent prostate cancer cells compared with their androgen-dependent counterparts (26,27,29), a finding that implicates heightened NF-κB activation as a contributing factor in the emergence of androgen independence.

Given that NF-κB transcriptionally regulates expression of genes involved in apoptosis and proliferation, it is not surprising that NF-κB activation would play a critical role in prostate carcinogenesis. Indeed, activation of NF-κB in prostate cancer specimens correlates with intratumoral expression of Bcl-2 and cyclin D1, two proteins that regulate survival and G_1-S-phase progression, respectively (25). Accordingly, our findings that PE exposure induced apoptosis and reduced proliferation in our *in vitro* and xenograft models strongly supports the notion that the NF-κB-inhibitory effect of PE is critical in mediating the growth-suppressive effects of PE.

Dietary agents with preventive potential can be applied at various points in the natural and treated history of prostate cancer. For example, in addition to primary prevention, pomegranate consumption could potentially be used to prevent or delay *clinical* recurrences once patients experience *biochemical* recurrences (PSA recurrences) after radical prostatectomy. Indeed, a recent phase II trial showed that consumption of PJ by patients who had experienced a PSA recurrence after radical prostatectomy prolonged the PSA doubling time by a factor of nearly 4-fold (11). It should be emphasized that although PJ was shown to slow PSA doubling times in our phase II trial, no pomegranate formulation has been shown to delay or prevent *clinical* recurrences. The results of our phase II trial has led to the initiation of a phase III placebo-controlled, randomized study to determine whether intake of PJ can lengthen the PSA doubling time in patients with a post-prostatectomy biochemical recurrence.

The results reported in our xenograft experiments involved the use of a dose of PE that was equivalent to approximately 10 times the dose that would be administered to a 70 kg human. Our study was done in such a manner as to seek proof-of-principle evidence that PE could modulate NF-κB activity and androgen-independent prostate cancer growth *in vivo*. Thus, one cannot necessarily extend our findings to the clinical setting until adequate, scientifically rigorous human trials are done. Although we have recently reported on the safety of PE in humans delivered over 4 weeks (35), the safety and tolerability of high doses of PE over extended durations have not been established.

Extending the duration of the androgen-dependent state could potentially prolong life expectancy of prostate cancer patients and delay or prevent the need for additional hormonal therapy or chemotherapy. In this regard, our finding that PE delayed the growth and emergence of androgen independence in our xenograft model may be particularly germane.

Of importance, our group showed previously that dietary fat reduction delayed the emergence of androgen independence and prolonged survival using a similar xenograft model (36). Future research will focus on potential additive and/or synergistic effects of combining a low-fat diet with PE. Based on our results, we propose that PJ could have potential as a dietary agent to prevent the emergence of androgen independence and suggest that this may be a high priority area for future clinical investigation.

Acknowledgments

Grant support: Sence Foundation and POM Wonderful (A. Pantuck), University of California-Los Angeles Prostate Specialized Program of Research Excellence grant P50 CA92131, and Department of Defense award W81XWH-04-1-0529 and Department of Veterans Affairs Merit Review Program (M.B. Rettig).

References

1. Kohnen PW, Drach GW. Patterns of inflammation in prostatic hyperplasia: a histologic and bacteriologic study. J Urol 1979;121:755–60. [PubMed: 88527]
2. De Marzo AM, Marchi VL, Epstein JI, Nelson WG. Proliferative inflammatory atrophy of the prostate: implications for prostatic carcinogenesis. Am J Pathol 1999;155:1985–92. [PubMed: 10595928]
3. Baldwin AS Jr. Series introduction: the transcription factor NF-κB and human disease. J Clin Invest 2001;107:3–6. [PubMed: 11134170]
4. Karin M, Cao Y, Greten FR, Li ZW. NF-κB in cancer: from innocent bystander to major culprit. Nat Rev Cancer 2002;2:301–10. [PubMed: 12001991]
5. Rayet B, Gelinas C. Aberrant rel/nfkb genes and activity in human cancer. Oncogene 1999;18:6938–47. [PubMed: 10602468]
6. Nair A, Venkatraman M, Maliekal TT, Nair B, Karunagaran D. NF-κB is constitutively activated in high-grade squamous intraepithelial lesions and squamous cell carcinomas of the human uterine cervix. Oncogene 2003;22:50–8. [PubMed: 12527907]
7. Greten FR, Eckmann L, Greten TF, et al. IKKβ links inflammation and tumorigenesis in a mouse model of colitis-associated cancer. Cell 2004;118:285–96. [PubMed: 15294155]
8. Pikarsky E, Porat RM, Stein I, et al. NF-κB functions as a tumour promoter in inflammation-associated cancer. Nature 2004;431:461–6. [PubMed: 15329734]
9. Domingo-Domenech J, Mellado B, Ferrer B, et al. Activation of nuclear factor-κB in human prostate carcinogenesis and association to biochemical relapse. Br J Cancer 2005;93:1285–94. [PubMed: 16278667]
10. Fradet V, Lessard L, Begin LR, et al. Nuclear factor-κB nuclear localization is predictive of biochemical recurrence in patients with positive margin prostate cancer. Clin Cancer Res 2004;10:8460–4. [PubMed: 15623625]
11. Pantuck AJ, Leppert JT, Zomorodian N, et al. Phase II study of pomegranate juice for men with rising prostate-specific antigen following surgery or radiation for prostate cancer. Clin Cancer Res 2006;12:4018–26. [PubMed: 16818701]
12. Ahmed S, Wang N, Hafeez BB, Cheruvu VK, Haqqi TM. *Punica granatum* L. extract inhibits IL-1β-induced expression of matrix metal-loproteinases by inhibiting the activation of MAP kinases and NF-κB in human chondrocytes *in vitro*. J Nutr 2005;135:2096–102. [PubMed: 16140882]
13. Afaq F, Malik A, Syed D, et al. Pomegranate fruit extract modulates UV-B-mediated phosphorylation of mitogen-activated protein kinases and activation of nuclear factor κB in normal human epidermal keratinocytes paragraph sign. Photochem Photobiol 2005;81:38–45. [PubMed: 15493960]
14. Schubert SY, Neeman I, Resnick N. A novel mechanism for the inhibition of NF-κB activation in vascular endothelial cells by natural antioxidants. FASEB J 2002;16:1931–3. [PubMed: 12368228]
15. Chen CD, Welsbie DS, Tran C, et al. Molecular determinants of resistance to antiandrogen therapy. Nat Med 2004;10:33–9. [PubMed: 14702632]

16. Patel BJ, Pantuck AJ, Zisman A, et al. CL1-GFP: an androgen independent metastatic tumor model for prostate cancer. J Urol 2000;164:1420–5. [PubMed: 10992426]
17. An J, Rettig MB. Epidermal growth factor receptor inhibition sensitizes renal cell carcinoma cells to the cytotoxic effects of bortezomib. Mol Cancer Ther 2007;6:61–9. [PubMed: 17237266]
18. Seeram NP, Henning SM, Zhang Y, et al. Pomegranate juice ellagitannin metabolites are present in human plasma and some persist in urine for up to 48 hours. J Nutr 2006;136:2481–5. [PubMed: 16988113]
19. Kreja L, Seidel HJ. On the cytotoxicity of some microbial volatile organic compounds as studied in the human lung cell line A549. Chemosphere 2002;49:105–10. [PubMed: 12243325]
20. Chen CD, Sawyers CL. NF-κB activates prostate-specific antigen expression and is upregulated in androgen-independent prostate cancer. Mol Cell Biol 2002;22:2862–70. [PubMed: 11909978]
21. Aggarwal BB, Shishodia S. Molecular targets of dietary agents for prevention and therapy of cancer. Biochem Pharmacol 2006;71:1397–421. [PubMed: 16563357]
22. Seeram NP, Aronson WJ, Zhang Y, et al. Pomegranate ellagitannin-derived metabolites inhibit prostate cancer growth and localize to the mouse prostate gland. J Agric Food Chem 2007;55:7732–7. [PubMed: 17722872]
23. Klein KA, Reiter RE, Redula J, et al. Progression of metastatic human prostate cancer to androgen independence in immunodeficient SCID mice. Nat Med 1997;3:402–8. [PubMed: 9095173]
24. Sartippour MR, Seeram NP, Rao JY, et al. Ellagitannin-rich pomegranate extract inhibits angiogenesis in prostate cancer *in vitro* and *in vivo*. Int J Oncol 2008;32:475–80. [PubMed: 18202771]
25. Shukla S, MacLennan GT, Fu P, et al. Nuclear factor-κB/p65 (Rel A) is constitutively activated in human prostate adenocarcinoma and correlates with disease progression. Neoplasia 2004;6:390–400. [PubMed: 15256061]
26. Gasparian AV, Yao YJ, Kowalczyk D, et al. The role of IKK in constitutive activation of NF-κB transcription factor in prostate carcinoma cells. J Cell Sci 2002;115:141–51. [PubMed: 11801732]
27. Suh J, Payvandi F, Edelstein LC, et al. Mechanisms of constitutive NF-κB activation in human prostate cancer cells. Prostate 2002;52:183–200. [PubMed: 12111695]
28. Palayoor ST, Youmell MY, Calderwood SK, Coleman CN, Price BD. Constitutive activation of IκB kinase α and NF-κB in prostate cancer cells is inhibited by ibuprofen. Oncogene 1999;18:7389–94. [PubMed: 10602496]
29. Shukla S, MacLennan GT, Marengo SR, Resnick MI, Gupta S. Constitutive activation of PI3K-Akt and NF-κB during prostate cancer progression in autochthonous transgenic mouse model. Prostate 2005;64:224–39. [PubMed: 15712212]
30. Huang S, Pettaway CA, Uehara H, Bucana CD, Fidler IJ. Blockade of NF-κB activity in human prostate cancer cells is associated with suppression of angiogenesis, invasion, and metastasis. Oncogene 2001;20:4188–97. [PubMed: 11464285]
31. Muenchen HJ, Lin DL, Walsh MA, Keller ET, Pienta KJ. Tumor necrosis factor-α-induced apoptosis in prostate cancer cells through inhibition of nuclear factor-κB by an IκBα "super-repressor. Clin Cancer Res 2000;6:1969–77. [PubMed: 10815922]
32. Pajonk F, Pajonk K, McBride WH. Inhibition of NF-κB, clonogenicity, and radiosensitivity of human cancer cells. J Natl Cancer Inst 1999;91:1956–60. [PubMed: 10564680]
33. Lindholm PF, Bub J, Kaul S, Shidham VB, Kajdacsy-Balla A. The role of constitutive NF-κB activity in PC-3 human prostate cancer cell invasive behavior. Clin Exp Metastasis 2000;18:471–9. [PubMed: 11592304]
34. Andela VB, Gordon AH, Zotalis G, et al. NFκB: a pivotal transcription factor in prostate cancer metastasis to bone. Clin Orthop Relat Res 2003;415:S75–85. [PubMed: 14600595]
35. Heber D, Seeram NP, Wyatt H, et al. Safety and antioxidant activity of a pomegranate ellagitannin-enriched polyphenol dietary supplement in overweight individuals with increased waist size. J Agric Food Chem 2007;55:10050–4. [PubMed: 17966977]
36. Ngo TH, Barnard RJ, Anton T, et al. Effect of isocaloric low-fat diet on prostate cancer xenograft progression to androgen independence. Cancer Res 2004;64:1252–4. [PubMed: 14973081]

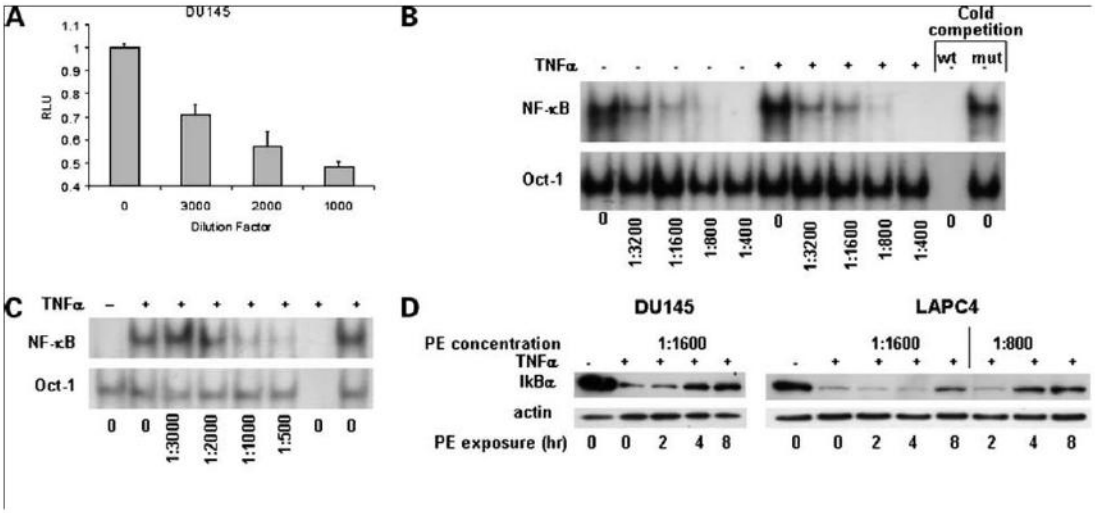

Figure 1.

PE inhibits constitutive and TNF-α-induced NF-κB activation. **A,** inhibition of constitutive NF-κB-driven reporter gene expression. Cells were plated in a 24-well format in triplicate and transiently transfected with a κB-luc reporter as well as the pRL-SV40 reporter for normalization of transfection efficiency. Cells were exposed to the indicated dilutions of PE for 24 h before harvesting of protein. Mean ± SD. **B,** EMSA showing PE-mediated inhibition of constitutive and TNF-α-induced (10 ng/mL × 30 min) NF-κB in DU145 cells. *Top,* NF-κB EMSA; *bottom,* Oct-1 EMSA. Lanes at far right show cold competition experiments with cold wild-type (*wt*) and mutant (*mut*) probes. Cells were exposed to indicated dilutions of PE for 4 h. **C,** same as **B** but in CL1 cells. **D,** *top,* Western blotting shows effects of PE on total IκBα levels in DU145 and LAPC4 cells after exposure to TNF-α; *bottom,* Western blot for actin as a protein loading control.

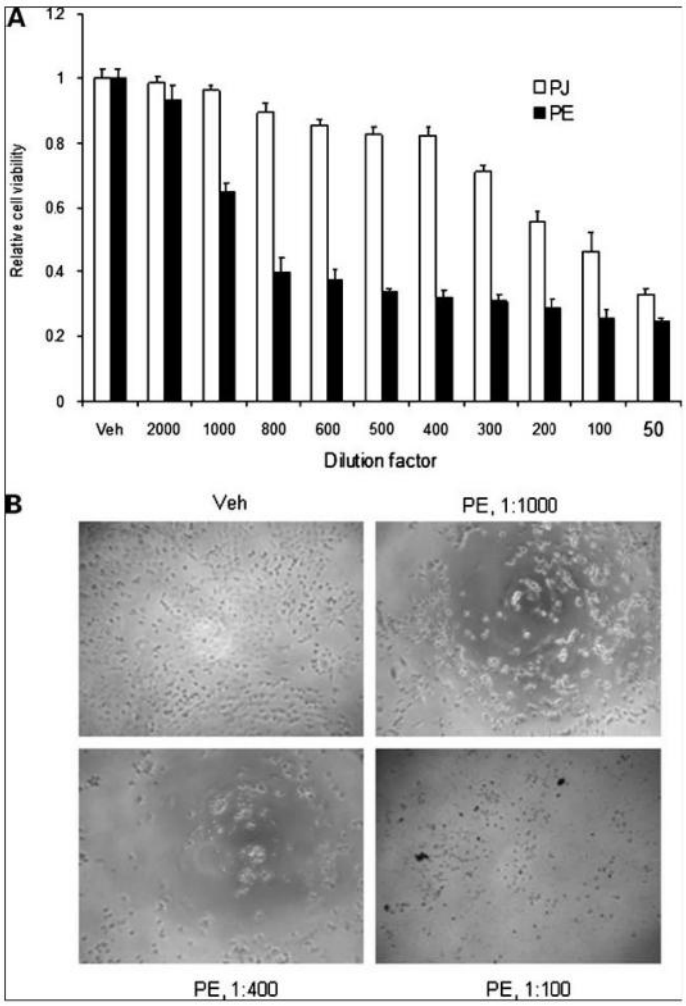

Figure 2.

Dose-dependent *in vitro* cytotoxicity of PE. **A,** DU145 cells were exposed to either PE or concentrated PJ at the indicated dilutions for 48 h and overall cell viability was measured by the methylene blue assay. Mean ± SD of four wells and were normalized to results of vehicle (PBS)-treated cells. **B,** photomicrographs of DU145 cells treated with the indicated dilutions of PE. Final magnification, ×200.

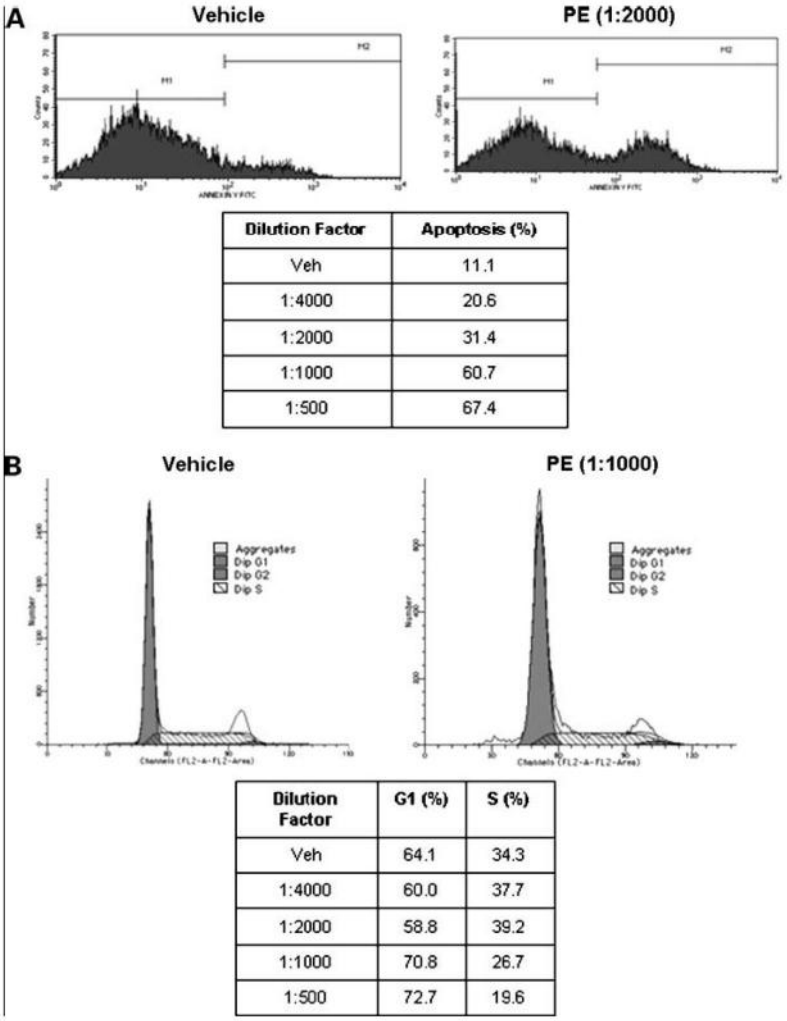

Dilution Factor	Apoptosis (%)
Veh	11.1
1:4000	20.6
1:2000	31.4
1:1000	60.7
1:500	67.4

Dilution Factor	G1 (%)	S (%)
Veh	64.1	34.3
1:4000	60.0	37.7
1:2000	58.8	39.2
1:1000	70.8	26.7
1:500	72.7	19.6

Figure 3.

Effects of PE on apoptosis and cell cycle profile of DU145 cells. Cells were exposed to PE for 48 h and then assayed for apoptosis by Annexin V staining (**A**) and cell cycle profile by hypotonic propidium iodide staining (**B**). Representative flow cytometric results. Numeric results are depicted in table form for both Annexin and hypotonic propidium iodide staining.

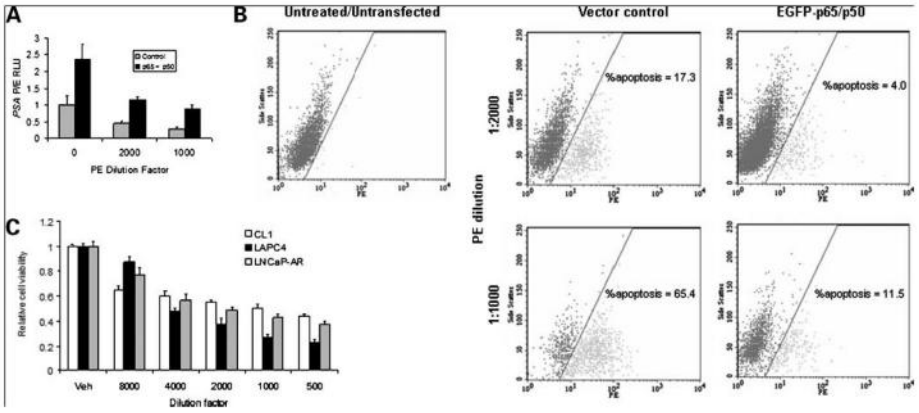

Figure 4.

PE-induced apoptosis is dependent on the NF-κB-inhibitory effect of PE. **A,** DU145 cells (0.8×10^5 per well in 24-well format) were transiently transfected with *PSA*-P/E-luc vector (1 μg) and the pEGFP-p65 and pCMV-p50 expression vectors (0.5 μg each). Twenty-four hours after transfection, PE (or PBS control) was added at the indicated dilutions for an additional 24 h before harvesting protein for reporter gene expression. Results were normalized to that of *Renilla* luciferase (pRL-SV40 cotransfected at 1 ng/well). Mean ± SD of three experiments. **B,** DU145 cells were plated in 10 cm dishes (1.5×10^6 per dish) and transfected with pEGFP-p65 and pCMV-p50 vectors (2.5 μg each). The next day, PE was added at the indicated dilutions and cells were harvested 24 h later. EGFP-positive cells were analyzed for apoptosis using a TUNEL assay as described in Materials and Methods. **C,** effects of PE on prostate cancer cell lines that lack constitutive NF-κB activation. Cells were exposed to the indicated dilutions of PE for 48 h and relative cell viability was determined. Mean ± SD of four wells and were normalized to results of vehicle (PBS)-treated cells.

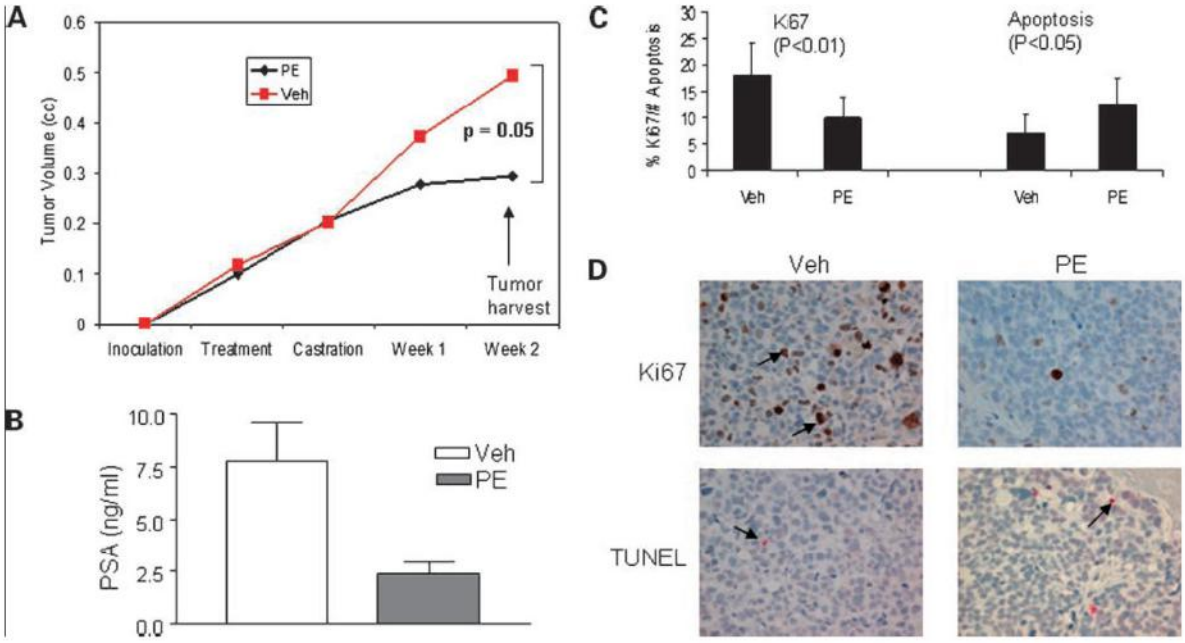

Figure 5.

Effects of PE on growth of androgen-independent mouse xenografts. After s.c. LAPC4 xenografts became palpable, mice were fed either PE or vehicle (*veh*) control ($n = 9$ for both groups) for 1 wk before castration followed by an additional 2 wk of dietary supplementation before euthanasia. **A,** tumor volumes in PE and vehicle-treated castrated mice. The mean tumor volume of the PE-treated group was statistically significantly smaller than that of the vehicle-treated group ($P = 0.05$, two-tailed Student's *t* test). **B,** serum PSA measurements in PE- and vehicle-treated animals at the time of sacrifice. **C** and **D,** proliferation is inhibited and apoptosis is induced in tumors in PE-treated compared with vehicle-treated mice. At the time of euthanasia, tumors were formalin-fixed and paraffin-embedded and subjected to either staining for the Ki-67 proliferation marker or for an apoptosis marker with the use of a TUNEL assay. **C,** mean of the percentage of cells that stain for Ki-67 and are positive for TUNEL staining based on counting of three representative high-power (×400) fields. **D,** representative photomicrographs of Ki-67 and TUNEL staining. Final magnification, ×200.

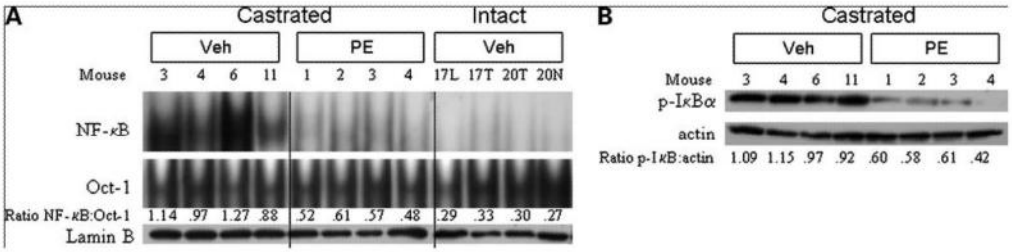

Figure 6.

PE inhibits NF-κB in androgen-independent LAPC4 xenografts. **A,** EMSA for NF-κB were done on nuclear protein extracted from frozen tumors taken at the time of euthanasia. *Top,* EMSA for NF-κB; *middle,* EMSA for Oct-1 as a control; *bottom,* Western blot for lamin B, a nuclear envelope protein, to show the integrity of our nuclear extracts and equality of protein loading. **B,** *top,* Western blot for phospho-IκBα; *bottom,* Western blot for actin as a protein loading control.